SYMMETRY-BASED MITOSIS DETECTION IN TIME-LAPSE MICROSCOPY

Topaz Gilad[⋆] *Mark-Anthony Bray*[†] *Anne E. Carpenter*[†] *Tammy Riklin Raviv*[⋆]

[⋆]Electrical and Computer Engineering Department, Ben-Gurion University of the Negev
[†] Imaging Platform, The Broad Institute of Harvard and MIT

ABSTRACT

Providing a general framework for mitosis detection is challenging. The variability of the visual traits and temporal features which classify the event of cell division is huge due to the numerous cell types, perturbations, imaging techniques and protocols used in microscopy imaging analysis studies. Therefore, the commonly used machine learning techniques that require specified sets of distinctive features along with a comprehensive set of training examples, are specific to particular datasets.

We present a robust mitotic event detection algorithm that accommodates the difficulty of the different cell appearances and dynamics. Addressing symmetrical cell divisions, we rely on the fact that the two daughter cells right after the division are approximately identical. Having detected pairs of candidate daughter cells, based on their association to potential mother cells, we look for the respective symmetry axes. We then calculate a similarity score for each of the selected pair of cells. The score functions as a likelihood measure for being a mitosis. Promising detection results for four different data sets of time-lapse microscopy imaging were obtained.

***Index Terms*—** Mitosis detection, Symmetry, Time-lapse Microscopy, High-throughput images

1. INTRODUCTION

Mitosis is the process in which the previously duplicated genetic material in a cell undergoes nucleus division. The study of mitosis (or cell division) has a substantial impact on many fields in the microbiology and biomedical world. Among them: the study of mutations and diseases, regenerative behaviors, cancer and metastasis, cell tracking and more. Time-lapse microscopy is an excellent platform to monitor cellular phenomena and events for a certain period of time. As technology develops and acquisition techniques advance, biologists face enormous amounts of data. Thus, the manual analysis of the images becomes impractical. As a result, the demand for elegant automatic tools for cell image analysis is ever growing.

1.1. Background and Related Work

Mitosis detection and cell tracking are intimately related. One can either use cell associations to detect cell devisions or use mitotic events as anchors for cell tracking. In [1] a mother cell is associated with one of the daughter cells, while the other daughter initiates a new track. Backward tracking is then performed to connect the two daughters with the mother cell. The main weakness of this strategy is the dependency of the mitosis detection quality on the tracking performances. Moreover, it requires an excessive computational complexity, when the purpose of the analysis is limited to the study of cell divisions. An alternative approach, if tracking is indeed needed, is to use the detected mitotic events which mark the initiation and the termination of cells path to guide the tracking. As the appearance of dividing cells can be changed dramatically, current approaches use machine learning algorithms, such as support vector machine (SVM), to detect mitotic events based on the visual and temporal traits [2, 3, 4]. While these methods are successful when sufficient positive training examples are available along with a carefully selected set of distinguishing features, they are impractical in general cases due to the huge variability in cells' dynamics and appearance, caused by the differences in datasets, the chemical compounds used, the microscopy imaging technique and the imaging parameters. For example, since mitosis is an extended process, composed of several distinctive stages, the rate of acquisition has significant implications on the extracted features.

1.2. Contribution

Consider the two pairs of consecutive frames, displayed in Figure 1, each showing mitosis of a different cell type acquired at a different rate. The proposed algorithm accommodates the difficulty of the different cell visual and temporal features without relying on the shape of the mother cell. Moreover, in contrast to most algorithms, it is not based on a full cell tracking, neither does it require a large amount of user annotated data. Instead, as the majority of cells undergo symmetrical divisions, we detect mitosis by measuring the similarity between the two daughter cells, right after the split. Using symmetry for mitosis detection has been suggested in [2], and applied to a data set of elongated cells, where the symmetry axis was determined based on the major axis of the mother cell. However, a symmetry axis is generally not as pronounced. Therefore, we suggest a novel algorithm to detect it based on our observation that the symmetry axis is orthogonal to the virtual straight line that connects the

Preprint submitted to 2015 IEEE International Symposium on Biomedical Imaging.
Received November 24, 2014.

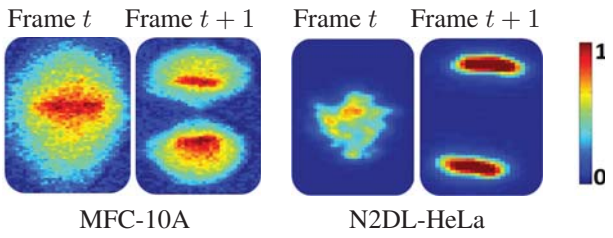

Fig. 1. Cell division from two different datasets: the mother cells are in frame t and the daughters in frame $t+1$. Each pair of daughter cells shows great similarity, although the datasets visually differ. Hereafter: 1. RGB colormap (instead of gray colormap) is used for highlighting. 2.MCF-10A dataset is courtesy of Albeck & Brugge. 3.N2DL-HeLa dataset source is [5, 6].

two daughter cells. We then quantify the level of 'asymmetry' based on shape similarity, if cell segmentation is given and reliable as well as a match between the gray-levels of the two sides. Encouraging detection rates were obtained for four different high-throughput microscopy datasets.

2. METHODS

The objective of the suggested method is a robust detection of mitotic events: Given a sequence of time-lapse microscopy images and their labeled segmentation, a list of detected mitotic events is formed. The algorithm consists of two main stages: mitotic candidate extraction using local mother-daughters relations, followed by examination of each candidate for mitosis by estimating a potential symmetry axis and calculating a similarity score between the candidate daughters. The score functions as a likelihood measure for being a mitosis.

2.1. Candidate selection

The goal of the first stage of the algorithm is to reduce the search space by creating a candidate list that will be further examined in the next stage for similarity between the candidate daughters. Therefore, that list should contain as much of the mitotic events, at the expanse of additional false positives (FP). The construction of the candidate list is performed according to mother-daughters spatial proximity: Let $I^t\colon \Omega_t \rightarrow \mathbb{R}$ define a gray level image frame acquired at time t where Ω^t is the $2D$ image domain. We define a candidate mother in frame t by $c_f^t,\ \ f=1,\ldots,F$ where F is the total number of detected cells in frame t. We search for candidate daughters in frame $t+1$ in the region defined by $\omega_f^{t+1} \triangleq \{(x,y) \in \Omega^{t+1} | (x-x_f)^2+(y-y_f)^2 \leq R^2\}$ where (x_f, y_f) are the center of mass (COM) coordinates of c_f^t and R is a predefined search radius that is estimated in a preliminary process from the sequence statistics. We denote by $\{c_{f,d_i}^{t+1}, c_{f,d_j}^{t+1}\}$ the pair of daughter cells candidates which relates to c_f^t, if found and if none of them is closer to the COM of a different mother. If more that two cells are detected in ω_f^{t+1}, then the nearest pair is selected. For now on, the superscript $t+1$ and the subscript f will be omitted for the sake of clarity.

2.2. Symmetry-based detection

Given a list of cell pairs, our objective is to detect the most likely daughter cells based on their similar appearance. Specifically, for each pair, we define a sub-image $I_{i,j}\colon \omega_{i,j} \rightarrow \mathbb{R}$, where $\omega_{i,j} \in \Omega$, which contains the two daughter cell candidates and measure its degree of bilateral symmetry. We assume that if such symmetry exists, the symmetry axis is perpendicular to the straight line that connects the COM of the daughter cells candidates and intersects it at its center. We define the intersection point by (x_0, y_0) and the angle of intersection by θ_0. However, note that, as cell segmentation might be inaccurate the calculated COMs could be erroneous. We therefore re-estimate the pose and orientation of the symmetry axis, as will be described shortly, and use (x_0, y_0) and θ_0 for initialization.

Symmetry axis detection: We estimate the symmetry axis of a sub-image $I_{i,j}$ containing two daughter cell candidates in the spirit of [7]. Let $J_{i,j}$ be the symmetrical counterpart of $I_{i,j}$ obtained (w.l.o.g.) by an up-down flip. Let R define a planar rotation matrix and let $\tau = [\tau_x, \tau_y, 1]$ be a translation vector defined using homogenous coordinate system. We look for the Euclidean transformation $H(\tau_x, \tau_y, \theta)$:

$$H(\tau_x, \tau_y, \theta) = [R; \tau] = \begin{bmatrix} \cos\theta & \sin\theta & \tau_x \\ -\sin\theta & \cos\theta & \tau_y \\ 0 & 0 & 1 \end{bmatrix} \quad (1)$$

that aligns $J_{i,j}$ to $I_{i,j}$. Formally, we solve the following optimization problem:

$$\{\hat{\tau_x}, \hat{\tau_y}, \hat{\theta}\} = \arg \max_{\tau_x, \tau_y, \theta} S_{sim}(I_{i,j}, H(\tau_x, \tau_y, \theta) \circ J_{i,j}), \quad (2)$$

where $J_{i,j}^H \triangleq H \circ J_{i,j}$ defines the transformation of $\omega_{i,j}$ (the image domain of $J_{i,j}$) by $H(\tau_x, \tau_y, \theta)$ and $S_{sim} \in [0,1]$ is a similarity score to be defined next. As shown in [7], the orientation of the symmetry axis is $\theta/2$ with respect to the coordinate system of $\omega_{i,j}$, and its midpoint coordinates are $\tau_x/2, \tau_y/2$, given that the origin of $\omega_{i,j}$ is located at its center. The concept is illustrated in Fig. 2.

Similarity score: Let $D_{i,j}$ be the binary label map (segmentation) of $I_{i,j}$, obtained by setting (w.l.o.g.) the image pixels that belong to the cell image to one and the background pixels to zero. Let $U_{i,j}$ be the symmetrical counterpart of $D_{i,j}$ (the flipped image) aligned by $H(\tau_x, \tau_y, \theta)$. We define a similarity score $S_{sim} \in [0,1]$ based on both the morphology and the gray level distribution of the two daughter cells candidates as follows:

$$\begin{aligned} S_{sim}(I_{i,j}, J_{i,j}^H) &= \alpha_1 S_{corr}(I_{i,j}, J_{i,j}^H) \\ &+ \alpha_2 S_{hist}(I_{i,j}, D_{i,j}) \\ &+ \alpha_3 S_{shape}(U_{i,j}, D_{i,j}), \end{aligned} \quad (3)$$

Preprint submitted to 2015 IEEE International Symposium on Biomedical Imaging.
Received November 24, 2014.

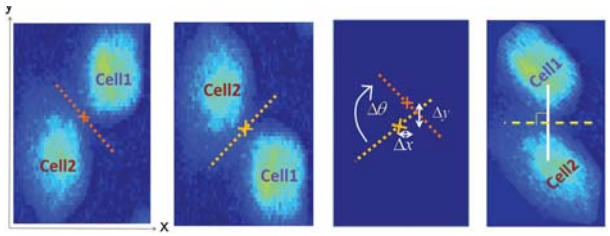

Fig. 2. Symmetry axis estimation (a) Original image. The symmetry axis is marked by a dashed line. Its midpoint is marked with a cross. (b) An up-down reflection of (a). (c) Symmetry axis and middle points of the initial image (in orange) and its reflection (in yellow). Parameters of the optimal H are in white. (d) After transforming the image using $\{\tau_x/2, \tau_y/2, \theta/2\}$ the symmetry axis is the horizontal axis that goes through the center of the sub image, and its midpoint coincides with the center of the transformed image.

where, $S_{corr}, S_{hist}, S_{shape} \in [0,1]$ are normalized similarity measures to be defined in the following and $\sum \alpha_i = 1$ are non-negative weights, that were the same for all the datasets.

Intensity correlation: The term S_{corr} could be obtained by a correlation between $I_{i,j}, J^H_{i,j}$. However, since, in dense environment, non-related cells can be captured in $I_{i,j}$ and break the symmetry, we use an approximated binary mask of the cells: $L_{i,j} = U_{i,j} \vee D_{i,j}$, where $\vee$ is the boolean operator OR. The score, S_{corr} is therefore the correlation result of $I_{i,j} \cdot L_{i,j}$ and $J^H_{i,j} \cdot L_{i,j}$ mapped to $[0,1]$.

In the case where the label maps (segmentations) are not reliable, then a weighted correlation can be used instead:

$$\begin{aligned} S_{corr}(I_{i,j}, J^H_{i,j}) &= \frac{\sigma_{ij}}{\sqrt{\sigma_{ii}\sigma_{jj}}}, \qquad (4) \\ \sigma_{ij} &= \frac{1}{N}\sum_{n=1}^{N} w_n (I^{(n)}_{i,j} - \overline{I_{i,j}})(J^{H,(n)}_{i,j} - \overline{J^H_{i,j}}) \\ \overline{I_{i,j}} &= \frac{1}{N}\sum_{n=1}^{N} w_n I^{(n)}_{i,j}, \quad \frac{1}{N}\sum_{n=1}^{N} w_n = 1. \end{aligned}$$

In fact, the weights w_n are the values of two $2D$ Gaussian functions $G^i(o^i, \sigma^i_x, \sigma^i_y)$ and $G^j(o^j, \sigma^j_x, \sigma^j_y)$, where the origins o^i, o^j are the COMs of each of the daughter cells, and the variances σ_x, σ_y are calculated based on the major axes of the cells. Therefore, lower weights are assigned to pixels that are distant from the approximated cell's center as the confidence they belong to the cell is lower. Figure 3 demonstrates the main concept.

Histogram matching: Let h_i, h_j be intensity histograms of I_{d_i} and I_{d_j}, respectively, where, I_{d_i} and I_{d_j}, are the scalar product of $I_{i,j}$ with the label maps (segmentations) of daughter i and daughter j respectively. Let $V = \{v\}$ define the range of a discretized gray level values in I_{d_i} and I_{d_j}. We define S_{hist} as follows:

$$S_{hist} = 1 - \frac{\sum_{v \in V} |h^v_i - h^v_j|}{\sum_{v \in V} \max(h^v_i, h^v_j)} \qquad (5)$$

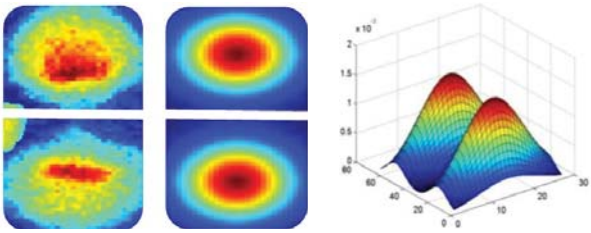

Fig. 3. Weights for correlation calculation: (a) Two daughter cells and additional cell that breaks the symmetry. (b) Colormaps representing w_n. (c) Two 2D Gaussians (mesh).

Shape similarity measures When the segmentation are reasonable reliable we can add to S_{sim} a measure of the overlap between daughter i and daughter j either by using either the Dice score [8]:

$$S_{dice}(D_{i,j}, U_{i,j}) = \frac{2(|D_{i,j}| \cap |U_{i,j}|)}{|D_{i,j}| + |U_{i,j}|}, \qquad (6)$$

or (and) the Jaccard measure:

$$S_{Jaccard}(D_{i,j}, U_{i,j}) = \frac{|D_{i,j}| \cap |U_{i,j}|)}{|D_{i,j}| \cup |U_{i,j}|}. \qquad (7)$$

3. EXPERIMENTS AND RESULTS

Experimental data: Four different datasets encompassing twelve microscopy sequences were examined: 1. N2DL-HeLa[1], see[5, 6] - HeLa cells stably expressing H2b-GFP, Olympus IX81 with plan 10x/0.4 objective lens, acquisition rate: 2 frames per hour (fph), resolution: 0.645×0.645 microns per pixel (mpp). 2. N2DH-SIM1 [5, 6] - simulated nuclei moving on a flat surface, resolution: 0.125×0.125 mpp. 3. N2DH-SIM+1 [5, 6]: Simulated nuclei of HL60 cells, rate 2 fph, resolution: 0.125×0.125 mpp. 4. A subset of MCF-10A2[2] cells expressing NLS-mCerulean and RFP-Geminin, wide-field epifluorescence, NikonTE2000, 20X objective, rate: 3fph and resolution: $0.2 - 0.3$ mpp.

The obtained list of mitotic events was compared to annotations of mitotic events provided by the ISBI challenge [5, 6]. Cell segmentation of the MCF-10A dataset, which was not part of the challenge, was performed via CellProfiler [9]. For

[1]Data source: V. Ulman and D. Svoboda, Centre for Biomedical Image Analysis, Masaryk University. Brno. Czech Republic (Created using Cytopacq).

[2]Data source: J. Brugge and J. Albeck

	#TP	#FP	#FN	Percision	Recall	F-Score
N2DH-SIM	104	5	12	95%	90%	92%
N2DH-HeLa	86	14	8	86%	91%	89%
N2DH-SIM+	62	1	5	98%	93%	95%
MCF-10A	10	1	2	91%	83%	87%

Table 1. Mitosis detection results for four different data sets.

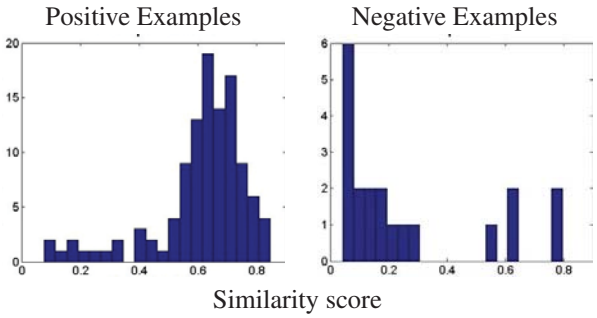

Fig. 4. Histograms of the similarity scores S_{sim} for the positive (left) and negative (right) examples, taken from the candidates list of the N2DH-SIM dataset [5, 6].

this sequence, we detected the mitotic events (for comparison with the automatic algorithm) by ourselves.

Results: Table 1 shows the quantitative results, which include the true positives (TP), false positives (FP), false negatives (FN), precision, recall and F-scores, for each of the tested datasets, from the pre-selected list of candidates. That list was selected such that the number of false negatives is zero on the expense of higher number of false positives; see Section 2.1 for details. Histograms of the similarity scores of the candidate list, obtained from the largest data set examined, are displayed in Figure 4. The similarity score S_{sim} allows good separation between the positive (mitotic events) and the negative cases. Nevertheless, there are a few examples of false detection (Figure 5). Addressing these outliers is a subject of future study, to be discussed next.

4. SUMMARY AND FUTURE DIRECTIONS

We presented a novel method for mitosis detection which overcomes the huge variability of high-throughput microscopy imaging of cells. This is accomplished by addressing symmetrical cell devisions and using symmetry as a guiding cue. High sensitivity and specificity measures were obtained for four different datasets of different sources.

Cells dynamics play an important role, distinguishing an actual cell division event from a random pair of cells passing by each other. Due to the forces of the microtubules in the mitotic spindle, pulling chromatin apart [10], the daughter cells appear as if they repel each other. This repulsion is captured within a frame or two after the splitting. Tracking the daughters, while measuring their relative distance and direction may provide additional useful information. Higher separability between positive and negative examples can be obtained by constructing a multi-dimension similarity score using both dynamic and appearance.

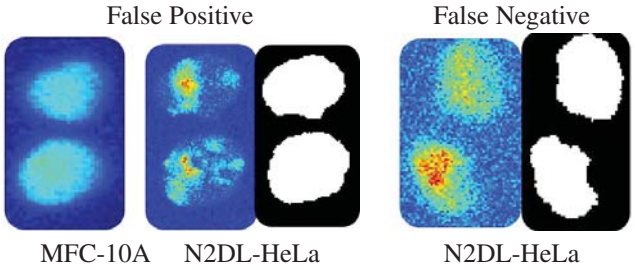

Fig. 5. Examples of false detection (left) and mis-detection in MFC-10A and N2DL-HeLa [5, 6] datasets.

Accurate segmentation is a key to improved mitosis detection, facilitating symmetry axis estimation and allowing more adequate similarity scores. Accurate association of the mother and daughters enhances the selection of the initial list of daughter candidates and improves motion detection. Therefore, current study focuses on the incorporation of the mitosis detection within a unified cell segmentation and tracking framework.

5. REFERENCES

[1] K. Thirusittampalam, M.J. Hossain, O. Ghita, and P.F. Whelan, "A novel framework for cellular tracking and mitosis detection in dense phase contrast microscopy images," *IEEE J. Biomedical and Health Informatics*, vol. 17, no. 3, 2013.

[2] F. Li, X. Zhou, J. Ma, and S.T.C. Wong, "Multiple nuclei tracking using integer programming quantitative cancer cell cycle analysis," *IEEE TMI*, vol. 29, no. 1, pp. 96–105, 2010.

[3] S. Huh, *Toward an Automated System for the Analysis of Cell Behavior: Cellular Event Detection and Cell Tracking in Time-lapse Live Cell Microscopy*, Ph.D. thesis, Carnegie Mellon University, March 2013, PhD thesis.

[4] A.A. Liu, K. Li, and T. Kanade, "A semi-markov model for mitosis segmentation in time-lapse phase contrast microscopy image sequences of stem cell populations," *IEEE TMI*, vol. 31, no. 2, pp. 359–369, 2012.

[5] M. Maska et al., "A benchmark for comparison of cell tracking algorithms," *Bioinformatic*, vol. 30, no. 11, pp. 1609–1617, 2014.

[6] C. Ortiz-de Solorzan, "Isbi 2014 cell tracking challenge," 2014, [Online; accessed 19-July-2014].

[7] T. Riklin Raviv, N. Sochen, and N. Kiryati, "On symmetry, perspectivity, and level-set based segmentation," *IEEE TPAMI*, vol. 31, no. 8, pp. 1458–1471, 2009.

[8] L. Dice, "Measure of the amount of ecological association between species," *Ecology*, vol. 26, no. 3, pp. 297–302, 1945.

[9] L. Kamentsky et al., "Improved structure, function, and compatibility for cellprofiler: modular high-throughput image analysis software," *Bioinformatics*, vol. 27, no. 8, 2011.

[10] D. Sadava, D.M. Hillis, H.C. Heller, and M.R Berenbaum, *Life: The Science of Biology*, 10th ed., 2012.

Preprint submitted to 2015 IEEE International Symposium on Biomedical Imaging.
Received November 24, 2014.